Enhanced Thermoelectric Power Factor of Na_xCoO_2 Thin Films by Structural Engineering

*Peter Brinks, Bouwe Kuiper, Eric Breckenfeld, Gertjan Koster, Lane W. Martin, Guus Rijnders, and Mark Huijben**

Increasing interest in thermoelectric energy generation for the direct conversion of thermal gradients into electrical power has intensified the search for new thermoelectric materials with enhanced conversion efficiency. The main challenge to improve the efficiency of the thermoelectric generation process is to independently control the electronic and thermal material properties.[1] Furthermore, due to the presence of extensive waste heat at elevated temperatures in many application areas, high chemical and structural stability of thermoelectric materials at high temperatures is an important requirement.[2] Among the most promising materials for high-temperature applications are the layered cobaltites, such as Na_xCoO_2, due to the high-temperature stability of complex oxide materials.[3] An optimum in the combined thermoelectric properties (i.e., Seebeck coefficient, electrical conductivity, and thermal conductivity) has been reported by the dimensionless figure of merit, *ZT*, for single crystals of Na_xCoO_2 at 800 K with *ZT* values of 1.2.[4] Increased disorder in polycrystalline Na_xCoO_2 samples reduced the electrical conductivity and thereby a reduced *ZT* value of 0.3 at 800 K was obtained.[4] To enable the application of this promising layered cobaltite in thermoelectric energy generators significant improvement in the thermoelectric properties is required.

Further enhancement of the *ZT* value can be achieved by an increase in Seebeck coefficient and electrical conductivity or a decrease in thermal conductivity. Due to the inverse proportionality of the charge carriers alterations (e.g., electrons) on the different thermoelectric properties, previous studies have focused on the suppression of phonon transport by the implementation of nanostructures to lower the thermal conductivity.[5] The independent control of the electronic and thermal material properties has successfully resulted in the improvement of telluride materials for low-temperature applications.[6] However, the enhanced reactivity of such nanostructured materials hampers the use of this approach for applications at elevated temperatures. An alternative approach is to use high-quality thin films, instead of bulk samples, in which structural engineering can be used to tune the specific thermoelectric material properties.

Detailed thermoelectric characterization of Na_xCoO_2 thin films has been hindered by the chemical instability in ambient conditions.[7,8] However, a recently developed method to obtain chemically stable, single-phase Na_xCoO_2 thin films by pulsed laser deposition due to the in situ deposition of an amorphous AlO_x capping layer enables us to exploit the intrinsic properties of these thermoelectric thin films.[8] Here, we show that by structural engineering in chemically stable Na_xCoO_2 thin films the thermoelectric properties can be controlled and enhanced as compared to bulk samples. By changing the single crystalline substrate material we can control the structural properties and as a consequence the electronic and thermal properties of the thermoelectric thin films. Tuning of the grain size within the Na_xCoO_2 thin films significantly influences the achievable Seebeck coefficient. We demonstrate that preservation of the crystallinity in these thin films with enhanced Seebeck coefficient results in minimal reduction of the electrical conductivity and, therefore, leads to a doubling of the thermoelectric power factor at room temperature.

Here, structural engineering is applied as a tool to obtain improved control over the thermoelectric properties of Na_xCoO_2 thin films, which is unique for epitaxial thin films and cannot be obtained in single crystal or polycrystalline samples. To study this effect, Na_xCoO_2 thin films were grown by pulsed laser deposition (PLD) on various single crystal substrates. All Na_xCoO_2 thin films were deposited under the same conditions and have a thickness of 60 nm. Independent of the substrate material and structure, all thin films showed a preferred growth orientation with the (00l) direction parallel to the surface normal.

Previously it was shown that the crystallinity of Na_xCoO_2 thin films does not strongly depend on the deposition temperature,[8] and an optimum deposition temperature of 430 °C was determined. However, the effect of oxygen deposition pressure on the crystallinity was not systematically studied yet. Here, we observe a significant decrease in crystallinity when the deposition pressure was reduced by one and two orders of magnitude from the previously reported value of 0.4 mbar,[8] resulting in an increased resistivity by a factor of five, together with a strong reduction of the Seebeck coefficient. Based on these results we can conclude that, although the deposition pressure can clearly be used to tune the crystallinity of these Na_xCoO_2 thin films, it will not provide the required enhanced control over the thermoelectric properties. Therefore the optimized deposition parameters[8] are used, which result in a combination of the optimum crystallinity and thermoelectric properties. Furthermore, all thin films have been cooled down after growth in 1 atm. of oxygen at a rate of 10 °C min^{-1} to optimize the oxidation level.

P. Brinks, B. Kuiper, Dr. G. Koster,
Prof. G. Rijnders, Dr. M. Huijben
MESA+ Institute for Nanotechnology
University of Twente
P.O. BOX 217, 7500 AE, Enschede, The Netherlands
E-mail: m.huijben@utwente.nl
E. Breckenfeld, Dr. L. W. Martin
Department of Materials Science and Engineering
and Materials Research Laboratory
University of Illinois
Urbana, IL 61801, USA

DOI: 10.1002/aenm.201301927

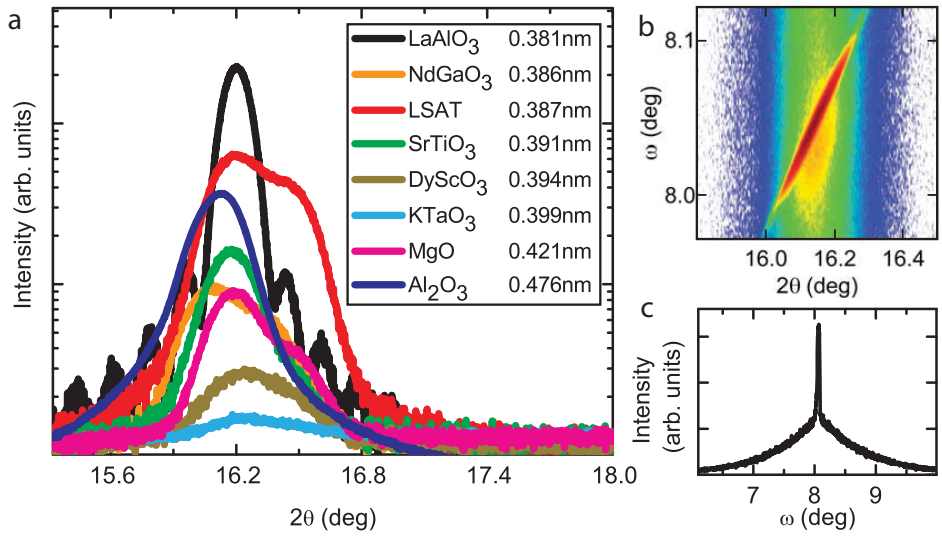

Figure 1. a) X-ray diffraction spectrum of the (002) diffraction peak of Na_xCoO_2 thin films deposited on different single crystal substrates. The corresponding lattice parameters of the substrates are indicated as well. b) 2θ vs. ω map scan of the Na_xCoO_2 (002) diffraction peak for a thin film deposited on LSAT. This scan reveals the presence of a sharp and a diffuse peak at the same 2θ angle and a small shift in ω angle. c) Rocking curve (ω scan) through the center of the peak at a 2θ value of 16.1°, showing the presence of a combination of a diffuse and a sharp peak.

This will provide similar oxygen stoichiometry in all thin films with a negligible amount of oxygen vacancies.

In **Figure 1**a the (002) Na_xCoO_2 diffraction peak is shown for thin films grown on different single crystal substrates. The differences in peak height indicate changes of the crystallinity of the thin films depending on the substrate material. The highest crystallinity is observed for the $LaAlO_3$ substrate, as confirmed by the observed Kiessig fringes around the main peak. These Kiessig fringes can only be observed in the case of a highly ordered crystal structure with a well-defined thickness and sharp interfaces. Thin films deposited on $(LaAlO_3)_{0.3}(Sr_2AlTaO_6)_{0.7}$ (LSAT) substrates exhibit the smallest reduction of crystallinity, although an additional peak is observed. This double peak is present in several thin films and is investigated in more detail for the thin film deposited on LSAT. A 2θ vs. ω map scan is shown in Figure 1b for the Na_xCoO_2 thin film deposited on LSAT, which reveals the presence of a sharp peak and a diffuse peak, which is even more clearly visible in the inset, where a rocking curve (ω scan) is shown. The 2θ position of the two peaks is similar, whereas for the ω position there is a small deviation, indicating that the two peaks are originating from crystalline parts with the same lattice constant but a small tilt angle with respect to each other. This behavior is indicative for the formation of misfit dislocations in heteroepitaxial systems with a relatively large lattice mismatch as previously reported for different thin films and superlattice systems.[9] A relation between the *c*-axis length of the crystal structure and the sodium concentration has been proposed for single crystal samples, where a shortening of the *c*-axis indicates a higher sodium concentration in the unit cell.[10–14] Because both observed peaks correspond to one *c*-axis lattice constant, these measurements indicate that the formation of misfit dislocations depends on the choice of substrate material and that the composition of the samples remains similar and is approximately $Na_{0.67}CoO_2$ for these thin films.[12] This is supported by in situ X-ray photoelectron spectroscopy (XPS) measurements (not shown), which show the same sodium to cobalt ratio for samples deposited on Al_2O_3, $LaAlO_3$, and LSAT substrates.

Previous studies have reported the growth of Na_xCoO_2 thin films on hexagonal (0001) Al_2O_3 as well as on cubic (001) $LaAlO_3$ and (001) $SrTiO_3$ single crystal substrates.[7,8,15–19] However, limited information is available on the crystalline ordering between the thin films and the underlying substrate. The weak in-plane ordering of the thin films on various substrates hampered detailed characterization by XRD. Therefore in situ X-ray photoelectron diffraction (XPD) experiments were performed. XPD provides element specific and surface sensitive information on the intrinsic crystal ordering of the Na_xCoO_2 surface. Stereographic projections of the oxygen 1s core level intensity maps are shown in **Figure 2**a. XPD measurements were done using 60 nm Na_xCoO_2 thin films deposited on Al_2O_3, $LaAlO_3$ and LSAT substrates, without a capping layer.

Strong in-plane ordering is confirmed for the growth of the hexagonal Na_xCoO_2 crystal structure on the hexagonal Al_2O_3 substrate. Clear 6-fold symmetry is observed, which is in good agreement with previous reports based on XRD measurements.[8,16,18,19] For the thin films grown on the cubic $LaAlO_3$ and LSAT substrates 12-fold symmetry is observed, suggesting two possible orientations in which the 6-fold symmetric Na_xCoO_2 is oriented. These variations in in-plane symmetries can be clearly observed in the additional phi-scans (Figure 2c). Based on the peak positions and additional information from XRD measurements regarding the in-plane substrate orientation, the in-plane crystallographic ordering of the Na_xCoO_2 thin films on the different substrates was determined. This orientation is schematically shown in Figure 2b, where it should be noted that for the cubic substrates the Na_xCoO_2 *a*-axis can be rotated by 15° in either direction, as compared to the *a*-axis of the substrate. Based on these measurements it can be

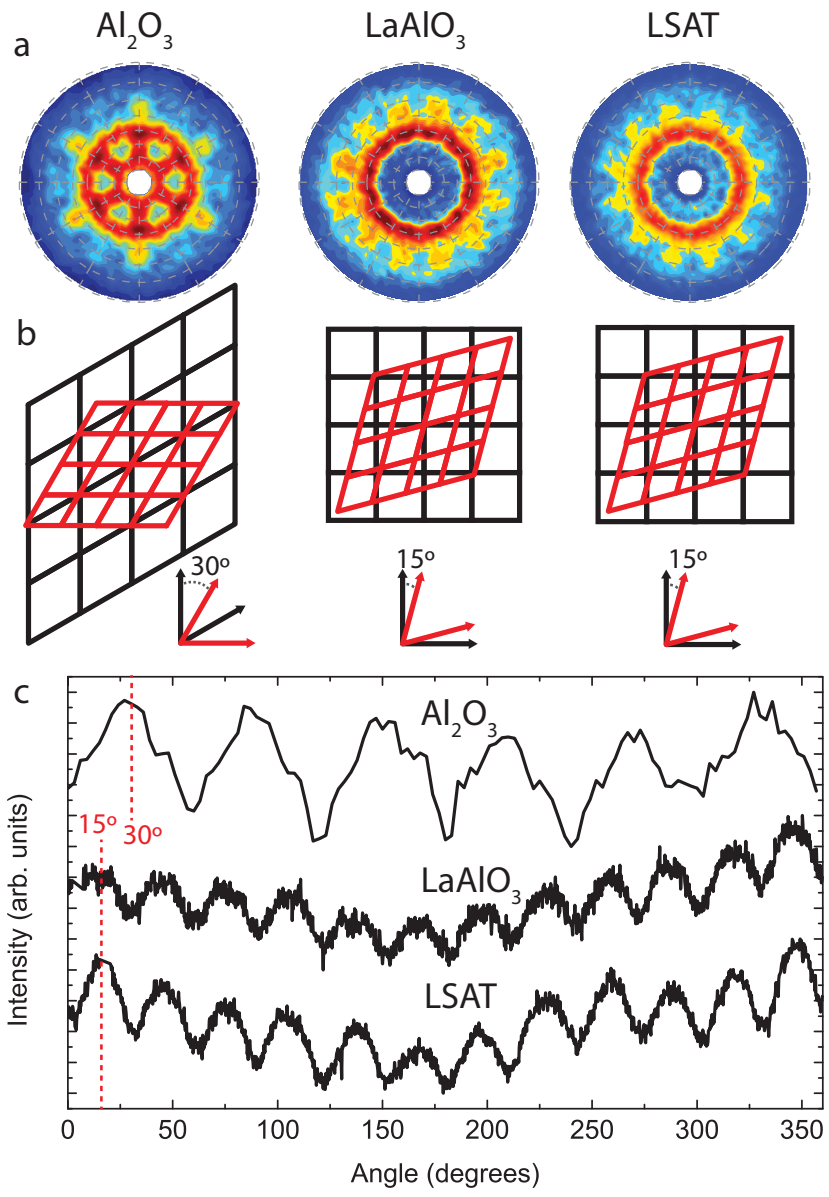

Figure 2. a) Oxygen 1s XPD intensity maps of Na_xCoO_2 thin films deposited on Al_2O_3, $LaAlO_3$ and LSAT single crystal substrates. b) Schematic representation of the in-plane ordering of the crystal structure of Na_xCoO_2 thin film on the specific substrate. The substrate and film structures are shown in black and red. c) Phi-scan at the peak position of the XPD map, revealing in-plane 6- or 12-fold symmetry of the Na_xCoO_2 thin films.

concluded that the growth of Na_xCoO_2 thin films is crystallographically ordered on cubic as well as hexagonal substrates, however, different levels of crystallinity are achieved. When these Na_xCoO_2 thin films are grown on the different (pseudo) cubic substrates, the level of crystal ordering in the thin films will be dependent on the lattice parameter of the substrate. It is expected that the variation in crystal ordering has a strong influence on the electronic and thermal properties of the thin films. Therefore, this method of structural engineering provides a direct control of the thermoelectric properties.

The dependence of the electronic and thermal properties of the Na_xCoO_2 thin films on the structural control by choice of single crystal substrate has been studied in detail. The resistivity as a function of temperature for various Na_xCoO_2 thin films is shown in **Figure 3**a. It can be clearly observed that all thin films show metallic behavior down to low temperatures, indicating the minimal effect of the strongly suppressed crystallinity (Figure 1a) on the electronic properties. The electrical conductivity and Seebeck coefficient for these thin films at room temperature are shown in Figure 3c as a function of the substrate crystal lattice parameter. Although no clear trend is visible for the electrical conductivity as a function of substrate lattice parameter, the highest electrical conductivity is observed in thin films with the highest crystallinity on substrates of Al_2O_3, $LaAlO_3$ and LSAT. From Hall measurements in a Van der Pauw geometry a constant carrier density in all thin films in the range between 1.9 and 3.3 × 10^{21} cm^{-3} was determined at room temperature by fitting to a single band model. Therefore, at room temperature the substrate dependence on the variation in electrical conductivity in the Na_xCoO_2 thin films is dominated by the carrier mobility, which is determined by the crystallinity, or defect density, strongly affecting the scattering processes. We observe a linear increase of the Hall resistance as a function of temperature between 150 and 300 K, as is shown in figure 3b. This is in good agreement with previous observations in single crystals[20] and thin films[8] and with theoretical predictions based on the *t–J* model, which take the strong electron correlations in Na_xCoO_2 into account, as well as the two-dimensional nature of the triangular CoO_2 layers.[21,22] These models predict a relatively constant Hall resistance in the low temperature regime and a linear increase of the Hall resistance in the high temperature regime. For our thin films we observe in addition to this linear increase at high temperature, a relatively constant Hall resistance below 150 K, consistent with the models. For thin films on Al_2O_3, $LaAlO_3$ and LSAT, we see a different behavior below 50 K, which resembles the observations in single crystals, in which even a change of sign for the Hall resistance is observed at the transition from the paramagnetic to the antiferromagnetic state (T_n = 21 K in single crystals).[20] We do not observe a change of sign, indicating that in our thin films the Néel temperature is significantly lowered because of the reduction in crystalline ordering as compared to single crystals.

The specific choice of a LSAT substrate showed the smallest decrease in crystallinity as compared to a thin film on a $LaAlO_3$ substrate. However, a significant enhancement of the Seebeck coefficient to values above 100 μV K^{-1} was observed, as shown

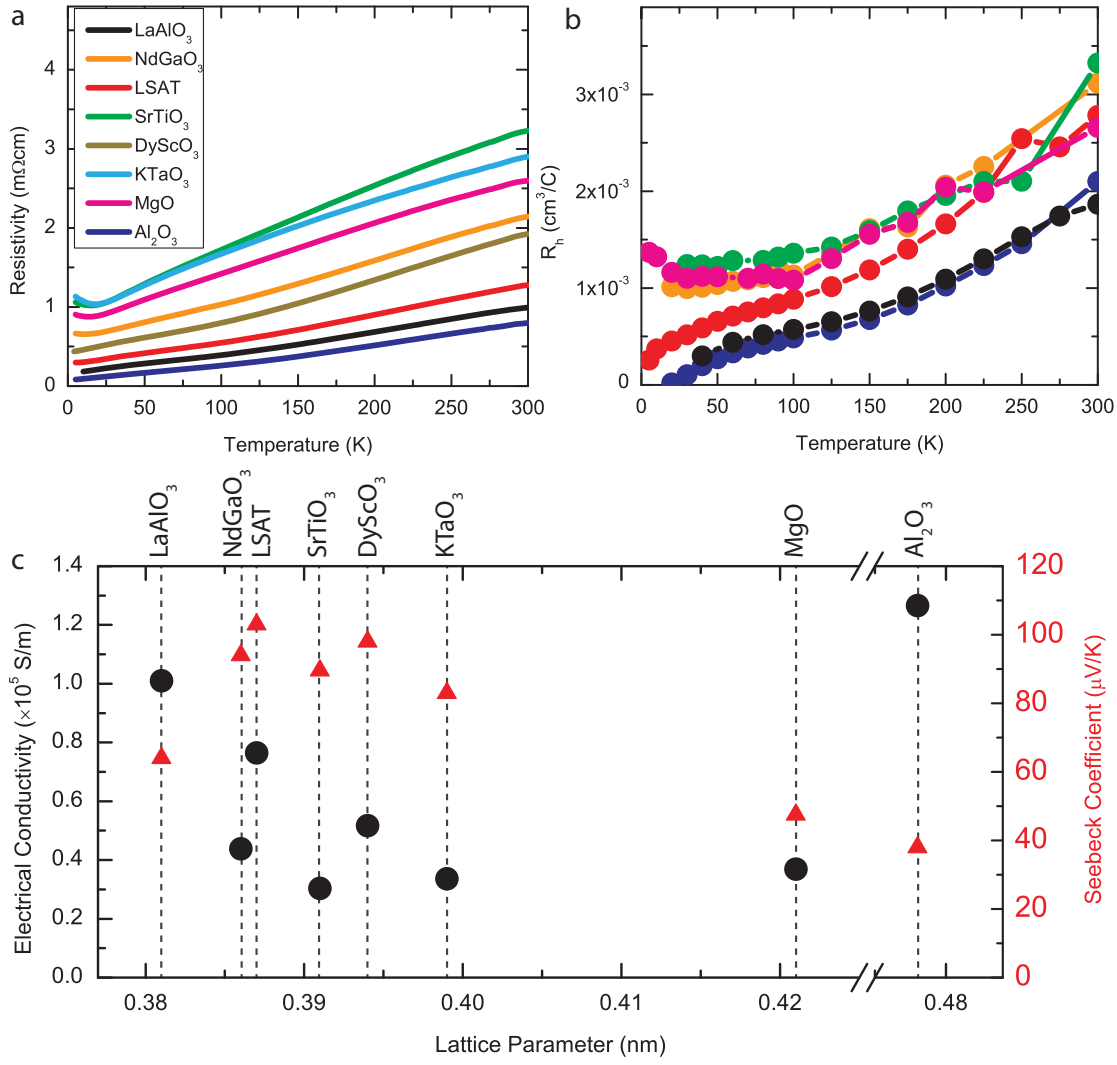

Figure 3. a) Resistivity as a function of temperature for Na_xCoO_2 thin films deposited on different substrates, showing metallic behaviour down to low temperatures for all samples. b) Corresponding temperature dependent Hall resistance values. c) Room temperature conductivity and Seebeck coefficient for these thin films as a function of substrate lattice parameter.

in Figure 3c, as compared to the previously reported value of about 70 μV K^{-1}.[8] As the difference in substrate lattice parameter does not provide a direct connection between crystal structure and enhancement of the Seebeck coefficient, the thin films have been characterized by atomic force microscopy (AFM) (**Figure 4**). It is apparent that the thin films have an increased surface roughness of 4–7 nm from the original substrate surfaces exhibiting a grainy surface structure. The surface morphology of the thin films is depending on the used substrate material. The average in-plane grain size is determined from fast Fourier transformation (FFT) spectra of the AFM images (Figure 4). These measurements show that, in addition to controlling the crystallinity, the grain size (microstructure) of these thin films can be controlled by changing the substrate material, enabling structural engineering of the Na_xCoO_2 thin films. The effect of variation in grain size on the Seebeck coefficient of the Na_xCoO_2 thin films is shown in **Figure 5**. It can be clearly seen that for thin films with a reduced grain size the Seebeck coefficient is significantly enhanced. This is in good agreement with reports of PbTe polycrystalline samples with a small grain size.[23] In these PbTe systems the enhancement of the Seebeck coefficient is suggested to be caused by carrier trapping at the grain boundaries.[24]

These newly engineered Na_xCoO_2 thin films with reduced grain sizes provide an optimal combination of thermoelectric properties, as the thin film with the smallest grain size only shows a minor reduction in crystallinity and, therefore, only a slight reduction of the electrical conductivity. Together with an enhanced Seebeck coefficient, this controlled structural engineering provides a promising direction for new thermoelectric materials. The combined results of the electrical conductivity and the Seebeck coefficient are shown in **Figure 6** where the thermoelectric power factor is plotted as a function of substrate lattice parameter. A doubling in power factor to 8.1 μW K^{-2} cm^{-1} can be observed for chemically stable Na_xCoO_2 thin films on LSAT substrates as compared to previously reported thin films

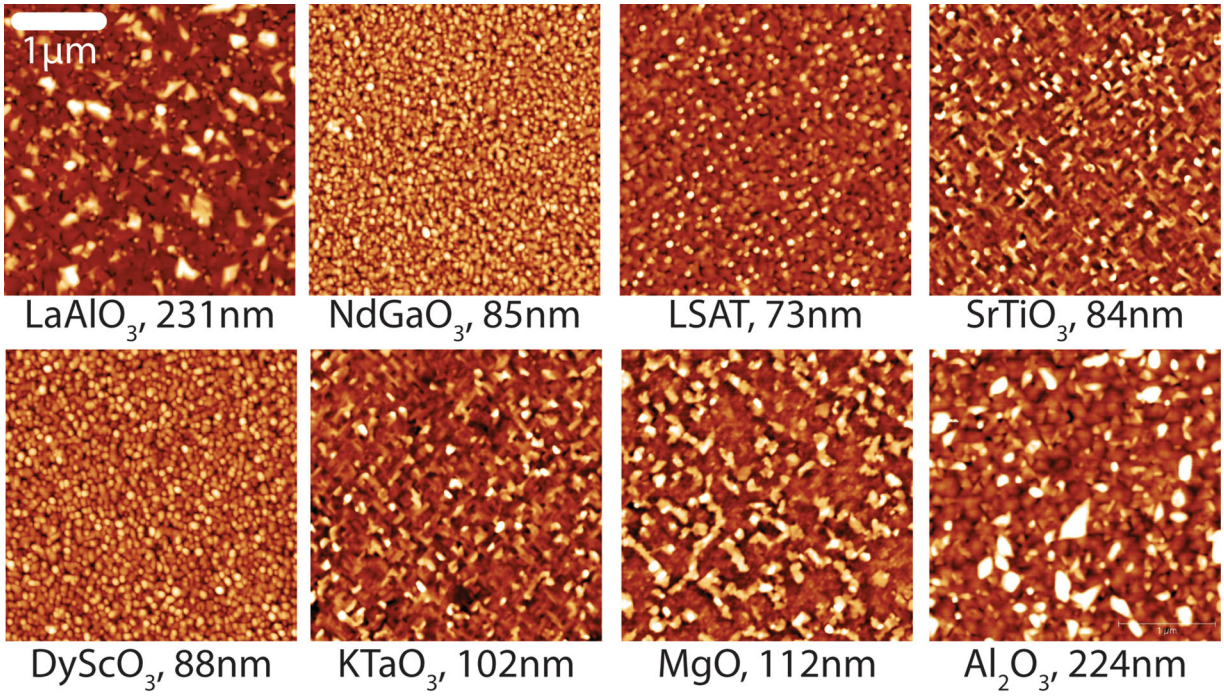

Figure 4. AFM images of capped Na_xCoO_2 thin films on various single crystal substrates, scan sizes 3 μm × 3 μm. The average in-plane grain size, based on a FFT spectrum of the AFM images, is given as well.

on $LaAlO_3$ and Al_2O_3 substrates.[8,14,18] Although this electronic performance is still lower than in single crystal samples with power factors up to 24 μW K^{-2} cm^{-1} at 300 K,[4,25] our structurally engineered thin films outperform polycrystalline samples which have power factors of only 6.0 μW K^{-2} cm^{-1}.[4,26]

To determine the effect of structural engineering on the thermal properties of the thin films, the thermal conductivity of several thin films was studied as well by time-domain-thermoreflectance measurements. For 100 nm thick films of Na_xCoO_2 on $LaAlO_3$ and LSAT the obtained room temperature thermal conductivity is 1.4 ± 0.1 W mK^{-1} for both samples, which is significantly lower than single crystalline and comparable with polycrystalline samples for which values of respectively 5–19 W mK^{-1}[4,25,27] and about 2.0 W mK^{-1}[4,26] are reported at room temperature for samples with similar compositions. A similar suppression of the thermal conductivity for samples with reduced grain size is previously reported for PbTe.[23] This indicates that structural engineering also provides control over the thermal properties in addition to the control of the electronic properties. These results clearly show a significant enhancement in the thermoelectric properties because of a simultaneous enhancement of the thermoelectric power factor and a reduction of the thermal conductivity. It should, however, be taken into account that the thermal conductivity is measured parallel to the surface normal (cross-plane), whereas the electronic properties are measured perpendicular to the surface normal

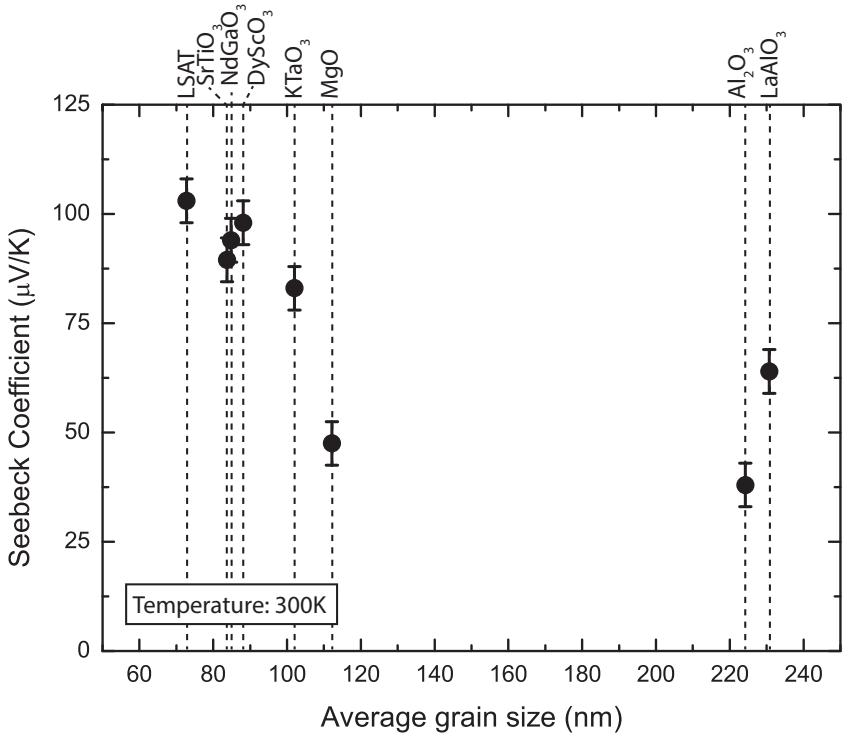

Figure 5. Room temperature Seebeck coefficient as a function of average in-plane grain size for Na_xCoO_2 thin films deposited on different single crystal substrates.

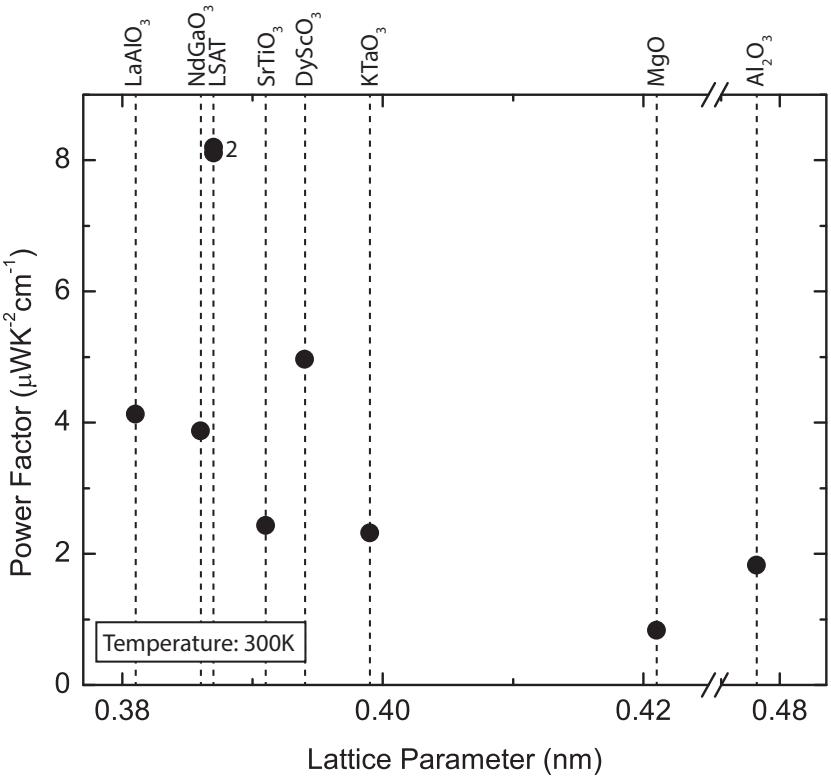

Figure 6. Power factor at 300K of Na_xCoO_2 thin films deposited on different single crystal substrates. A dramatic enhancement in power factor is observed for thin films deposited on LSAT substrates. The number 2 indicates two samples with values too close to distinguish the individual symbols in the graph.

(in-plane) and that it is therefore not correct to calculate *ZT* values based on these measurements. It can be concluded that this structural engineering is a very promising approach to improve the thermoelectric properties of Na_xCoO_2 thin films by simultaneously controlling the electronic as well as thermal properties.

We have studied the relation between structural and thermoelectric properties of Na_xCoO_2 thin films deposited on different single crystal substrates. For these thin films we show that hexagonal Na_xCoO_2 thin films can be deposited on various cubic as well as hexagonal single crystal substrates, with only a minimal loss of crystallinity, which is required to preserve the electrical conductivity. Additionally we demonstrate that by changing the substrate material we can reduce the in-plane average grain size, leading to a significant enhancement of the Seebeck coefficient. However, the influence of the ionic conductivity of Na_xCoO_2, which makes this also an interesting cathode material for battery applications,[10] has to be determined in more detail.

We show that by structural engineering, controlling crystallinity and grain size, in Na_xCoO_2 thin films, the electronic as well as thermal properties can be controlled. For the optimized Na_xCoO_2 thin films on LSAT substrates we observe a simultaneous doubling of the thermoelectric power factor and a strong suppression of the thermal conductivity, leading to a dramatic enhancement of the overall thermoelectric properties of our Na_xCoO_2 thin films at room temperature.

Experimental Section

Na_xCoO_2 thin films were grown by pulsed laser deposition (PLD) from a sintered target with a $Na_{0.9}CoO_2$ composition. Optimized growth parameters for the thin films and capping layer, as previously reported,[8] were used to prevent the formation of impurity phases and to ensure the chemical stability of the fabricated thin films. Additionally, the oxygen pressure during growth was varied in the range between 0.004 and 0.4 mbar to determine the dependence of the obtained crystallinity.

To enable structural engineering of the Na_xCoO_2 thin films various single crystal substrates were used with a large variation in lattice parameters of their corresponding crystal structures. All substrates were annealed to form low roughness surfaces with step-terrace structures exhibiting unit-cell height steps, as determined by AFM using a Bruker Dimension Icon. Al_2O_3, $(LaAlO_3)_{0.3}(Sr_2AlTaO_6)_{0.7}$ (LSAT) and MgO were annealed at a temperature of 1050 °C for, respectively, 1, 2, and 10 h. $LaAlO_3$, $NdGaO_3$, $SrTiO_3$ and $DyScO_3$ were annealed at a temperature of 950 °C for, respectively, 1, 2, 2, and 4 h and $KTaO_3$ was annealed for 2 h at a temperature of 500 °C. Structural properties of the thin films were characterized by XRD, using a Bruker D8 Discover diffractometer and a Panalytical X'Pert PRO MRD. To obtain additional in-plane structural information, XPD measurements were performed on an Omicron Nanotechnology XPS system, using a rotating sample setup with a fixed angle between the monochromatic Al Kα X-Ray source and the detector. The electronic properties were characterized by a Quantum Design PPMS system, while the room temperature measurements of the Seebeck coefficient were performed on a custom setup with an accuracy of 7% as determined with a Bi2Te3 reference sample (SRM3451) from the National Institute of Standards and Technology (NIST).[28] Thermal conductivity was determined for several thin films by time-domain-thermoreflectance measurements, which provides values for the thermal conductivity parallel to the surface normal (cross-plane).

Acknowledgements

M.H. and G.R. acknowledge support by the Netherlands Organization for Scientific Research (NWO). E.B. and L.W.M. acknowledge support from the National Science Foundation under grant DMR-1149062.

Received: December 15, 2013
Published online: February 12, 2014

[1] J. R. Sootsman, D. Y. Chung, M. G. Kanatzidis, *Angew. Chem. Int. Ed.* **2009**, *48*, 8616.
[2] H. Ohta, K. Sugiura, K. Koumoto, *Inorg. Chem.* **2008**, *47*, 8429.
[3] T. M. Tritt, M. A. Subramanian, *MRS Bull.* **2011**, *31*, 188.
[4] K. Fujita, T. Mochida, K. Nakamura, *Jpn. J. Appl. Phys.* **2001**, *40*, 4644.
[5] C. J. Vineis, A. Shakouri, A. Majumdar, M. G. Kanatzidis, *Adv. Mater.* **2010**, *22*, 3970.
[6] R. Venkatasubramanian, E. Siivola, T. Colpitts, B. O'Quinn, *Nature* **2001**, *413*, 597.
[7] H. Zhou, X. P. Zhang, B. T. Xie, Y. S. Xiao, C. X. Yang, Y. J. He, Y. G. Zhao, *Thin Solid Films* **2006**, *497*, 338.

[8] P. Brinks, H. Heijmerikx, T. A. Hendriks, G. Rijnders, M. Huijben, *RSC Adv.* **2012**, *2*, 6023.
[9] V. M. Kaganer, R. Köhler, M. Schmidbauer, R. Opitz, B. Jenichen, *Phys. Rev. B* **1997**, *55*, 1793.
[10] R. Berthelot, D. Carlier, C. Delmas, *Nat. Mater.* **2011**, *10*, 74.
[11] Y. Krockenberger, I. Fritsch, G. Christiani, H. U. Habermeier, L. Yu, C. Bernhard, B. Keimer, L. Alff, *Appl. Phys. Lett.* **2006**, *88*, 162501.
[12] Q. Huang, M. L. Foo, R. A. Pascal, Jr., J. W. Lynn, B. H. Toby, T. He, H. W. Zandbergen, R. J. Cava, *Phys. Rev. B* **2004**, *70*, 184110.
[13] L. Viciu, J. W. G. Bos, H. W. Zandbergen, Q. Huang, M. L. Foo, S. Ishiwata, A. P. Ramirez, M. Lee, N. P. Ong, R. J. Cava, *Phys. Rev. B* **2006**, *73*, 174104.
[14] X. P. Zhang, Y. S. Xiao, H. Zhou, B. T. Xie, C. X. Yang, Y. G. Zhao, *Mater. Sci. Forum* **2005**, *3807*, 475.
[15] L. Yu, L. Gu, Y. WANG, P. X. Zhang, H. U. Habermeier, *J. Cryst. Growth* **2011**, *328*, 34.
[16] J. Y. Son, *J. Phys. D: Appl. Phys.* **2008**, *41*, 095405.
[17] Y. Krockenberger, I. Fritsch, G. Cristiani, A. Matveev, L. Alff, H. U. Habermeier, B. Keimer, *Appl. Phys. Lett.* **2005**, *86*, 191913.
[18] A. Venimadhav, A. Soukiassian, D. A. Tenne, Q. Li, X. X. Xi, D. G. Schlom, R. Arroyave, Z. K. Liu, H. P. Sun, P. Pan, Xiaoqing, M. Lee, N. P. Ong, *Appl. Phys. Lett.* **2005**, *87*, 172104.
[19] J. Y. Son, B. G. Kim, J. H. Cho, *Appl. Phys. Lett.* **2005**, *86*, 221918.
[20] P. Mandal, P. Choudhury, *Phys. Rev. B* **2012**, *86*, 094423.
[21] B. Sriram Shastry, *Rep. Prog. Phys.* **2009**, *72*, 016501.
[22] W. Koshibae, A. Oguri, S. Maekawa, *Phys. Rev. B* **2007**, *75*, 205115.
[23] K. Kishimoto, T. Koyanagi, *J. Appl. Phys.* **2002**, *92*, 2544.
[24] J. Martin, L. Wang, L. Chen, G. S. Nolas, *Phys. Rev. B* **2009**, *79*, 115311.
[25] B. C. Sales, R. Jin, K. A. Affholter, P. Khalifah, G. M. Veith, D. Mandrus, *Phys. Rev. B* **2004**, *70*, 174419.
[26] K. Takahata, Y. Iguchi, D. Tanaka, T. Itoh, I. Terasaki, *Phys. Rev. B* **2000**, *61*, 12551.
[27] X. Tang, K. Aaron, J. He, T. M. Tritt, *Phys. Status Solidi A* **2008**, *205*, 1152.
[28] N. D. Lowhorn, W. Wong-Ng, Z. Q. Lu, E. Thomas, M. Otani, M. Green, N. Dilley, J. Sharp, T. N. Tran, *Appl. Phys. A* **2009**, *96*, 511.

